Extended Abstracts of the 2007 International Conference on Solid State Devices and Materials, Tsukuba, 2007, pp. 714-715

A-5-2

Electron Holography Characterization of Ultra-Shallow Junctions in 30-nm Gate-length MOS-FETs

Nobuyuki Ikarashi[1], Makiko Oshida[1], Makoto Miyamura[1], Motofumi Saitoh[1], Akira Mineji[2], and Seiichi Shishiguchi[2]
[1]NEC Corporation, Device Platforms Research Laboratories,
1120 Shimokuzawa, Sagamihara, 229-1198, Japan
Phone: +81-42-771-2458 E-mail: n-ikarashi@cq.jp.nec.com
[2] NEC Electronics Corporation, Process Technology Division,
1120 Shimokuzawa, Sagamihara, 229-1198, Japan

1. Introduction

A significant technical challenge in fabricating source/drain extensions (SDE) for advanced MOS-FETs is controlling the transient enhanced diffusion (TED) and the resultant redistribution of B during activation annealing [1]. Few techniques can be used to examine B distributions in the SDEs of scaled MOS-FETs [2- 4].

Electron holography can be used to map the electrostatic potential produced by dopants in semiconductors [2, 3, 5]. However, no quantitative investigations into the SDE regions of advanced MOS-FETs (45-nm technology node and beyond) using electron holography have been reported. This is probably due to surface damage caused by high-energy Ga ion bombardment during focused ion beam (FIB) thinning, which is usually used to prepare specimens for electron holography examination [6, 7].

We demonstrate that electron holography can be used to examine electrostatic potentials in the SDEs of 30-nm gate-length MOS-FETs. We quantitatively clarify the potential distributions in SDEs fabricated using two different implantation techniques (Ge+C+B co-implantation [8, 9] and conventional BF_2 implantation). Specimens were prepared by low-energy Ar ion milling to reduce surface damage. We also show that the measured potential distributions explain the electronic characteristics of the MOS-FETs.

2. Experiments

Samples

We examined the pMOS-FET SDEs that were formed using co-implantation or conventional BF_2 implantation. In the co-implantation process, C and B ions were implanted after Ge pre-amorphization of the substrate [9]. Secondary ion mass spectroscopy (SIMS) depth profiles of B implanted using these techniques are shown in Fig. 1. The B concentration drops sharply at a depth of 20 nm in the co-implantation sample, while it drops at a depth of 30 nm in the BF_2 sample.

Line-and-space-patterns (30-nm gate-length) were used in these examinations. The offset-spacer width was 4 nm in the co-implantation sample and 10 nm in the BF_2 implantation sample. This is because co-implantation was expected to suppress the short channel effect [9]. Devices were fabricated using the standard MOS-FET process (Fig. 2).

Electron holography

To reduce surface damage, we used low energy Ar ion milling instead of FIB thinning. The acceleration voltage was 3.5 kV or lower and the incident beam angle was 4°. The Ar ion beam was irradiated from the substrate-side (back-side) to avoid the curtain effect [6].

We used a JEOL 2010F transmission electron microscope equipped with an electron bi-prism. The spatial resolution determined on the basis of the sampling frequency in the phase reconstructions was 6.5 nm.

3. Results

Representative potential maps of the samples are shown in Fig. 3. Dark and bright areas correspond to p+ type regions and n type regions, respectively. We set potentials of the darkest (the brightest) areas to -0.5 V (+0.4 V).

We found that the 0.0-V equi-potential lines in the co-implantation sample were indented deeply at a depth of 20 nm. In contrast, no such indentations were observed in the BF_2 implantation sample. This indentation reflects the n-type region formed by halo implantation. Therefore, the potential maps show that B TED was well suppressed in the co-implantation sample, and the SDE regions (p+ type) and the halo regions (n-type) did not blur each other, while those regions in the BF_2 implantation sample blurred due to B TED in the depth direction. In addition, the depth of the indentation in the co-implantation sample (20 nm beneath the extension surface) was consistent with SIMS results (Fig. 1), which shows that the B concentration dropped sharply at a depth of 20 nm.

To investigate the B redistribution in parallel with the extension surface, we measured potential distributions in the channel direction at 10 nm beneath the extension surface (between the dotted white lines marked 10 nm in Fig 3). The measured potential line profiles in Fig. 4 show that the potential changed sharply within the offset-spacer edges in the co-implantation sample, while it changed gradually in the BF_2 implantation sample and the slopes ran over the edge; the distance from the offset-spacer edge to the position of the 0.0-V potential (indicated by arrows) was 7.6 nm in the former and 9.5 nm in the latter. This clearly shows that the B TED in the channel direction was suppressed more in the co-implantation sample.

Roll-off curves of our pMOS-FETs are shown in Fig. 5. The steep slopes match each other in the short gate-length region despite the thinner offset-spacer of the co-implantation sample. In addition, the reverse short channel effect was more clearly observed in the

co-implantation sample. These results were probably caused by the reduction of B redistribution and the resultant steeper potential change at the p-n junctions in the co-implantation sample, which are shown in Figs. 3 and 4.

3. Conclusion

Using electron holography, the potential distributions in the SDEs of 30-nm gate-length pMOS-FETs were quantitatively examined. To perform low-noise observations, specimens were prepared using back-side Ar ion milling (instead of FIB thinning) to reduce surface damage. Our analysis revealed the difference between the two-dimensional potential distribution in the SDEs formed by co-implantation and that in those formed by conventional BF_2 implantation, and indicated that the potential changed more steeply at the p-n junction in the former. We also showed that our holography results were consistent with the electronic characteristics of the MOS-FETs.

Acknowledgements

We thank Dr. T. Fukai for his helpful comments. We also thank Dr. H. Watanabe for his critical comments.

References

1. For example, N. E. B. Cowern, K. T. F. Janssen, and H. F. F. Jos, J. Appl. Phys. 68, 6191 (1990), and P. M. Fahey, P. B. Griffin, and J. D. Plummer, Rev. Mod. Phys. 61, 289 (1989).
2. N. Duhayona et el., J. Vac. Sci. Technol. B 22, 385 (2004).
3. Y. Y. Wang et al., Ultramicroscopy, 101, 63 (2004).
4. H. Fukutome, Y. Momiyama, E. Yoshida, M. Okuno, T. Itakura, and T. Aoyama, Tech. Digest IEDM 2005, 4 (2005).
5. M. R. McCartney, D. J. Smith, R. Hull, J. C. Bean, E. Voelkl and B. Frost, Appl. Phys. Lett. 65, 2603 (1994).
6. R. E. Dunin-Borkowski, S. B. Newcomb, T. Kasama, M. R. McCartney, and M. Weylanda, P. A. Midgley, Ultramicroscopy 103, 67 (2005).
7. M. R. McCartney et al., AIP Conf. Proc. 788, 565 (2005).
8. P. A. Stolk, D. J. Eaglesham, H.-J. Gossmann, and J. M. Poate, Appl. Phys. Lett. 66, 1370 (1995).
9. A. Mineji and S. Shishiguchi, IWJT Proc. 2006 84 (2006).

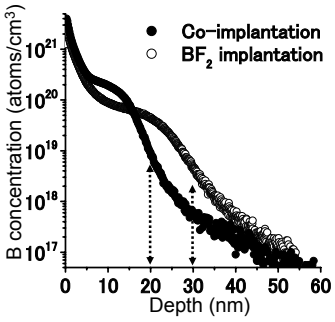

Fig. 1 SIMS depth profile of B implanted using co-implantation and BF_2 implantation

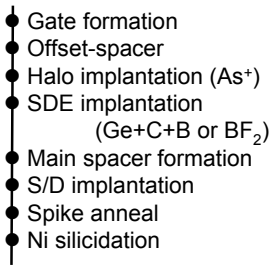

Fig. 2 Process flow of pMOS-FET fabrication.

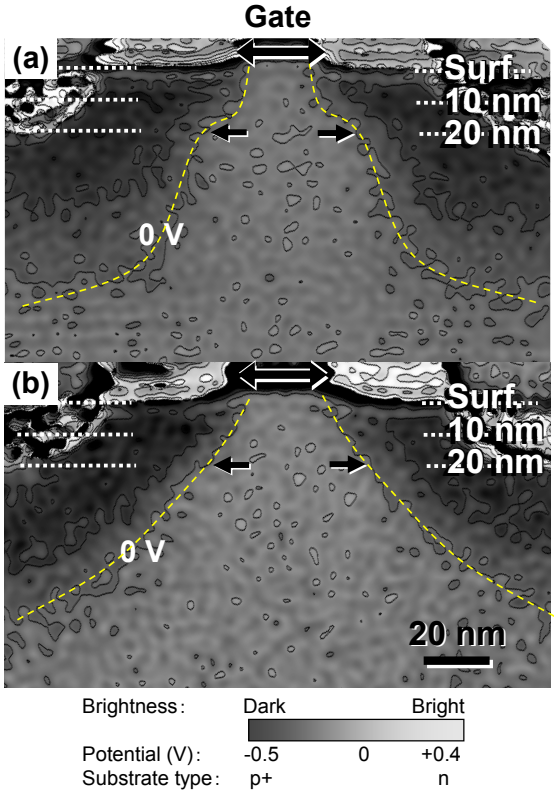

Fig. 3 Potential maps of (a) co-implantation sample (4-nm offset-spacer), and (b) BF_2 implantation sample (10-nm offset- spacer). 0.0-V equi-potential lines are traced with dotted curves for easy identification.

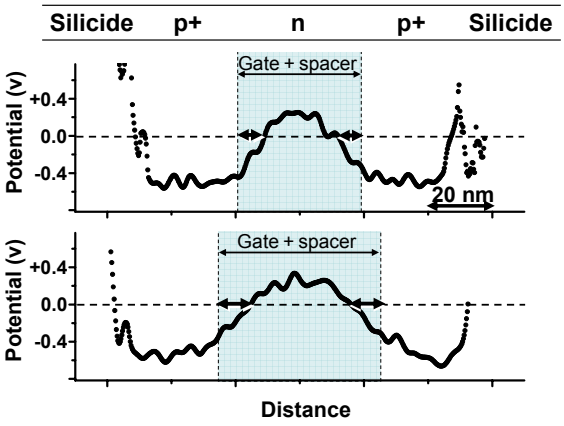

Fig. 4 Line profiles of potential distribution in channel direction (10 nm beneath extension surface) of (a) co-implantation sample and (b) BF_2 implantation sample. Vertical dotted lines show offset-spacer edges.

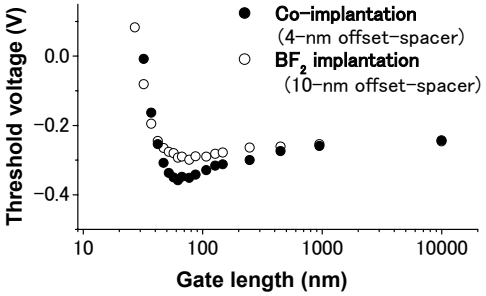

Fig. 5 Roll-off curves of samples. Steep slopes below 50 nm match each other. Reverse short channel effect (drop at 60 nm) occurred in co-implantation sample.